

Transmission through an Arbitrarily Shaped Aperture in a Conducting Plane Separating Air and a Chiral Medium

Ş. Taha İmeci¹, Fikret Altunkılıç², Joseph R. Mautz² and Ercüment Arvas²

¹ Vali İzzetbey Cad.,
KTO Karatay University, Karatay Medresesi Karşısı, Kemaliye Sok. No: 7
42030 Karatay – Konya – TURKEY
tahaimeci@halic.edu.tr

² Department of Electrical Engineering and Computer Science
Syracuse University, Syracuse, NY, 13244, USA
faltunki@syr.edu, jrmautz@syr.edu; earvas@syr.edu

Abstract- The analysis of chiral materials has been an important subject in computational electromagnetics. In this paper, the method of moments technique is used to solve the problem of transmission through an arbitrarily shaped aperture separating air and a chiral medium. The aperture is in an infinite PEC (perfect electric conductor) plane. The excitation is assumed to be a plane wave in air. The equivalence principle is used to replace the aperture with a conducting surface with an equivalent magnetic current on each side of it. By enforcing the continuity of the tangential components of the total electric and magnetic fields across the aperture, coupled integral equations are obtained. The aperture has been modeled by triangular patches. The equivalent magnetic currents are approximated by linear combinations of expansion functions. The mixed potential formulation for a homogeneous chiral medium is used to obtain the electric and the magnetic fields produced by these expansion functions. The coefficients of these expansion functions are obtained by using the method of moments to solve the coupled integral equations.

Index Terms- Apertures, chiral media, conductors, moment methods.

I. INTRODUCTION

In this work, an aperture problem is solved using some electromagnetic simulation tools and numerical analysis. More specifically, a numerical technique is used to solve an electromagnetic

transmission problem involving a chiral medium. Before the development of fast software and hardware technologies, analytical solutions were possible and popular for solving simple numerical electromagnetic problems. After the new era of computing tools arose, it was possible to do extensive numerical analysis to solve more electromagnetic problems especially those of transmission and/or scattering.

Numerical analysis of chiral materials has been done using a variety of numerical methods, such as the method of moments (MoM) [1], the finite-difference time-domain (FDTD) method [2], the finite element method-boundary element method (FEM-BEM) [3], and the transmission line modeling (TLM) method [4]. In this paper, a MoM formulation has been developed for chiral material and this formulation has been verified for transmission through an aperture by comparing the numerical results with other solutions. In Section II, the constitutive relations and the field of sources in an unbounded chiral medium are discussed. The basic formulation which leads to the detailed formulation in Section III is developed in Section II. Section IV contains numerical results and discussion. Some of the numerical results are compared with results obtained elsewhere. The conclusion and final comments are given in Section V.

II. CHIRAL MEDIA

The constitutive relations for a chiral medium are given in [5] as:

$$\bar{D} = \varepsilon \bar{E} - j\xi \bar{H} \quad (1)$$

$$\bar{B} = \mu \bar{H} + j\xi \bar{E} \quad (2)$$

where ε is the permittivity, μ is the permeability, and ξ is the chirality. These constitutive relations reduce to those for a simple dielectric medium when $\xi = 0$. A chiral material is defined by its constitutive relations (1) and (2). The constitutive relations (1) and (2) completely define the electromagnetic behavior of a chiral material.

The electromagnetic fields must satisfy the Maxwell equations given by

$$\nabla \times \bar{E} = -j\omega \bar{B} - \bar{M} \quad (3)$$

$$\nabla \times \bar{H} = j\omega \bar{D} + \bar{J}. \quad (4)$$

The field in a chiral medium is a right-handed field plus a left-handed field. In order to get Maxwell's equations for the right- and left-handed fields and current sources of the wavefield decomposition [1], [5], [6] one can put these constitutive relations into (3) and (4) and get that,

$$\nabla \times \bar{E}_{\pm} = -j\omega \mu_{\pm} \bar{H}_{\pm} - \bar{M}_{\pm} \quad (5)$$

$$\nabla \times \bar{H}_{\pm} = j\omega \varepsilon_{\pm} \bar{E}_{\pm} + \bar{J}_{\pm} \quad (6)$$

Equations (5) and (6) are called the equivalent Maxwell equations for the right-handed and left-handed fields. These equations, and hence their solutions, are very similar to those of sources radiating in an unbounded regular (achiral) medium. The mixed potential formulation [7] is used to obtain the fields of these kinds of sources.

III. 3-D VIEW OF THE PROBLEM AND FORMULATION

Figure 1 shows a plane wave, coming from the direction specified by θ^i and ϕ^i incident upon an arbitrarily shaped aperture in the PEC plane. This plane separates the half-space filled with air (ε_0, μ_0), from that filled with a homogeneous chiral medium ($\varepsilon_b, \mu_b, \xi$).

The equivalence principle [8], which is that for an achiral-achiral separation with one of the achiral mediums replaced by the chiral medium, is applied. An equivalent problem is obtained by closing the aperture with a PEC and placing magnetic currents $\pm \bar{M} = \pm \bar{E} \times \hat{z}$ immediately above and below the closed aperture as shown in Fig. 2. Continuity of $\bar{E} \times \hat{z}$ across the aperture is one

boundary condition that is satisfied by putting \bar{M} and $-\bar{M}$ in Fig. 2. Another boundary condition that must be satisfied is continuity of $\hat{z} \times \bar{H}$ across the aperture. By image theory, the field of \bar{M} above the PEC plane is that of $2\bar{M}$ in air. Figure 3 is for determining the field of $-\bar{M}$ in the chiral medium.

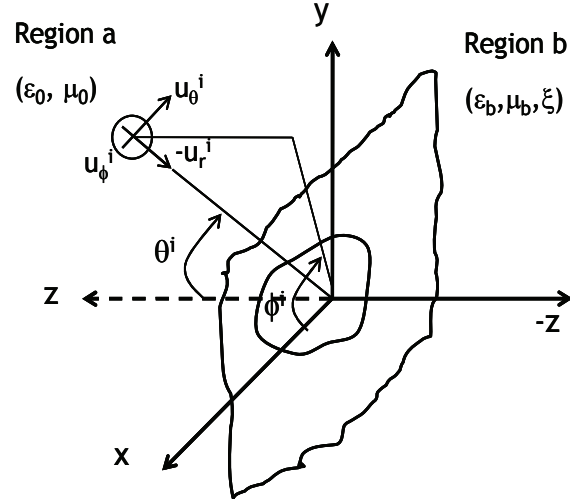


Fig. 1. Three dimensional depiction of the problem.

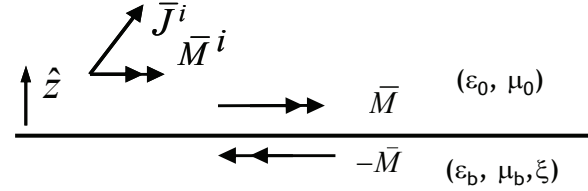


Fig. 2. Equivalence for regions a and b.

below the PEC plane in Fig. 2. If, in Fig. 2, radiation for $z > 0$ was not restricted to air and radiation for $z < 0$ was not restricted to the chiral medium, Fig. 2 would be valid for the separation of any two different mediums. In the image principle for a chiral medium, the image of the chiral medium is the chiral medium with the sign of its chirality changed. Therefore, application of the image principle does not result in a hypothetical situation where all space is filled with the same chiral medium. Instead of applying the image principle for a chiral medium, we deal with the infinite PEC plane directly. In order to apply the method of moments, we have to approximate the infinite PEC plane by a finite PEC plane. The finite PEC plane has to be so large that the electric current induced on it is nearly the same as the

electric current that would be induced on the infinite PEC plane. The effect of the finite PEC plane is that of the electric current \bar{J} that flows on it in Fig. 3. Of course, \bar{J} must be such that, on the finite PEC plane, the electric field of the combination of \bar{J} and $-\bar{M}$ has no component tangent to the PEC plane. Because there should be no field in Region a of Fig. 3, the medium in Region a of Fig. 3 is of no consequence. Liberty was taken to put the chiral medium (ϵ_b, μ_b, ξ) in Region a of Fig. 3.

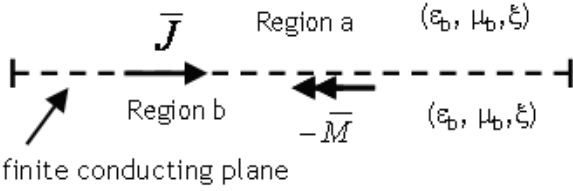


Fig. 3. Finite PEC plane just above $-\bar{M}$.

Now,

$$\bar{E}_{\tan}^b(\bar{J}, -\bar{M}) = 0 \quad (7)$$

just above $-\bar{M}$, on the whole finite PEC plane in Fig. 3, and continuity of the tangential magnetic field across the aperture in the original problem of Fig. 1 is expressed as,

$$2[\bar{H}_{\tan}^{inc} + \bar{H}_{\tan}^a(0, \bar{M})]_{z=0^+} = [\bar{H}_{\tan}^b(\bar{J}, -\bar{M})]_{z=0^-} \quad (8)$$

over the aperture. The superscript a indicates radiation in all space filled with the medium (ϵ_0, μ_0) of Region a, and the superscript b indicates radiation in all space filled with the medium (ϵ_b, μ_b, ξ) of Region b. Also, \bar{H}^{inc} is the free-space incident magnetic field. Although the left-hand side of (7) and the right-hand side of (8) are obtained by using the finite PEC plane, the left-hand side of (8) is, in view of application of the method of images, obtained by using the infinite PEC plane.

The left-hand side of (7) and the right-hand side of (8) could not be obtained by using the infinite PEC plane because the usual method of images does not apply to an infinite PEC plane in a chiral medium.

Equations (7) and (8) are solved for \bar{J} and \bar{M} by using the method of moments.

$$\bar{J}(\bar{r}) = \sum_{n=1}^{N'} I_n \bar{f}_n(\bar{r}) \quad (9)$$

$$\bar{M}(\bar{r}) = \sum_{n=1}^N V_n \bar{f}_n(\bar{r}) \quad (10)$$

where $\{\bar{f}_n(\bar{r}), n = 1, 2, \dots\}$ are the RWG [9] expansion functions, I_n and V_n are unknown coefficients to be calculated, N is the number of expansion functions in the aperture, and $N' =$ is the number of expansion functions on the whole finite PEC plane. RWG stands for the last names of the authors of [9].

The only difference between the equivalence principle where one or both regions are chiral and the equivalence principle where both regions are achiral is that in the equivalence principle where one or both regions are chiral, the equivalent currents radiate in the chiral region or regions. In the manuscript, the equivalence principle is merely applied; its derivation and explanation appears in [8].

Our MoM approach is not with a dyadic Green's function but with the mixed potential formulation. The dyadic Green's function approach for obtaining the electric field of an electric current involves an integral whose integrand contains the Green's function and its second order derivative. This integral is difficult to evaluate because its integrand is singular. In the mixed potential approach [7], there is an integral whose integrand contains the Green's function and there is the gradient of an integral whose integrand contains the Green's function. By manipulation, one can trade the gradient operation on the latter integral for the surface divergence operation on the MoM testing function and arrive at a formulation that is more suitable for computation than the dyadic Green's formulation.

It is difficult to obtain a good estimate of the error incurred by the use of a finite ground plane. We did a crude convergence study where we began with a small ground plane and made it larger and larger until the magnitude of the electric current near its edges was less than 11% of its maximum value in the vicinity of the magnetic current.

IV. NUMERICAL RESULTS

A. Square Aperture

Figure 4 shows a square conducting plate of side length 2λ . At its center is a square aperture of side length $L=0.25\lambda$. The plate and the aperture are modeled by triangular patches, with a finer mesh around the aperture. Figures 5–8 show currents $|M_y|$ and $|J_x|$ due to a normally incident plane wave traveling in the negative z -direction. The electric field of this plane wave is

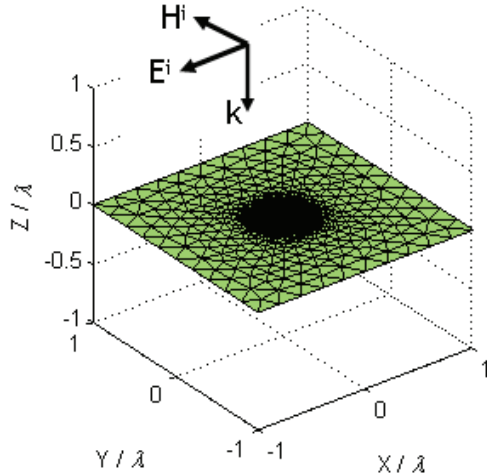


Fig. 4. Square aperture in a finite conducting plane.

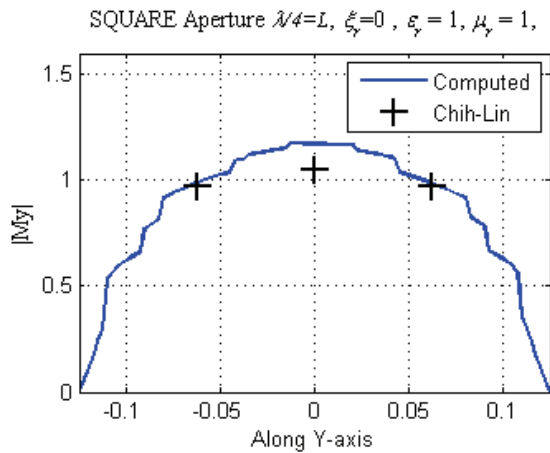


Fig. 5. Equivalent magnetic current when $\xi=0$.

$\vec{E}^{inc} = -\vec{a}_x E^{inc} e^{jk_z z}$. Figures 5 and 6 are for the special case where the chiral material is replaced by air (ϵ_0, μ_0). This case was considered to compare our results with those of [10]. In Figs. 5–10 the units along each horizontal axis are those of the ratio of length to wavelength. The

units of M_y are those of the incident electric field and the units of J_x are those of the incident magnetic field. The phase of M_y is plotted in degrees. Our computed results shown in Figs. 5 and 6 are in good agreement with [10].

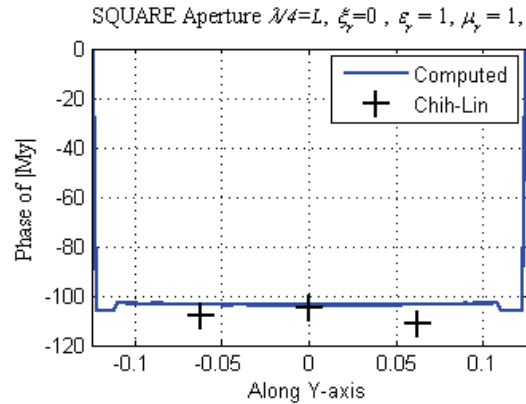


Fig. 6. Phase of equivalent magnetic current when $\xi=0$.

In [10], only 32 triangles were used in the aperture region while we have 241 triangles, and finer mesh around the edges. The finer mesh, easily obtainable with computational facilities of our day, should give better accuracy than that in [10]. For achiral media, the present approach still uses the finite PEC plane for radiation in the Region b half space whereas the approach in [10] uses an infinite PEC plane. For the achiral cases, agreement of results of the present approach with results in [10] therefore shows that, at least for these achiral cases, the finite PEC plane was large enough to be a good approximation of an infinite PEC plane. A 2254×2254 matrix was used. The computation time for a 4GHz processor machine in MATLAB was 16 minutes. Figure 7 shows the effect of chirality on the equivalent magnetic current in the aperture, and Fig. 8 shows J_x , the x-component of J , on the finite PEC plane. In Figs. 7 and 8, $\epsilon_r=2, \mu_r=1$ and $\xi_r = \xi / \sqrt{\mu\epsilon}$ where ϵ_r, μ_r and ξ_r are, respectively, relative permittivity, permeability and chirality of Region b. No results for comparison with the curves of Figs. 7 and 8 were available in the literature. We observe that as chirality gets smaller, the results in Fig. 7 seem to approach those in Fig. 5 despite the difference in

permittivities. In Fig. 8, $\eta_0 = \sqrt{\mu_0 / \varepsilon_0}$. It is noted that the current in Fig. 8 is very small as one moves away from the aperture by only half a wavelength. This is justification for approximating an infinite PEC plane with one that is a square of side length only 2λ .

Co-polarized and cross-polarized bistatic radar cross sections (RCS) are shown in Figs. 9 and 10. The co-polarized RCS is called $\sigma_{\theta\theta}$ because the incident electric field is θ -polarized and only the θ -component of the diffracted electric field is received. The RCS is a measure of the square of the magnitude of the diffracted field in Region a. The diffracted electric field is the electric field due to the aperture. That is, the diffracted electric field is the electric field that exists when the aperture is in the PEC screen minus the electric field that would exist if the aperture were not in the PEC screen. The cross-polarized RCS is called $\sigma_{\phi\phi}$ because the incident electric field is θ -polarized and only the ϕ -component of the diffracted electric field is received. For both Figs. 9 and 10, the excitation is a normally incident ($\theta^{inc}=0$) plane wave with its electric field polarized in the $-x$ -direction. In Fig. 9, the θ -component of the diffracted electric field is received at θ in the $\phi=0$ plane. In Fig.10, the ϕ -component of the diffracted electric field is received at θ in the $\phi=0$ plane. The ϕ component in the $\phi=0$ plane is the y component in the xz plane. All figures which have “along Y-axis” at the bottom are versus y/λ along the y-axis.

The internal field has been calculated along the z -axis, from the center of the aperture at $z/\lambda = 0$ down to $z/\lambda = -1$. The side length of the square aperture is $L = \lambda/4$ and the side length of the conducting plane is 2λ . The excitation is again a normally incident plane wave whose electric field is $\vec{E}^{inc} = -\vec{a}_x E^{inc} e^{jk_z z}$. Computed values are the magnitudes of $-E_x/E^{inc}$ and E_y/E^{inc} and their phases with and without chirality. In Fig. 11 where the chirality is zero, $|E_x/E^{inc}|$ approaches $|M_y/E^{inc}|$ in the aperture in Fig. 5. In Fig. 12 where the chirality is also zero, the phase of

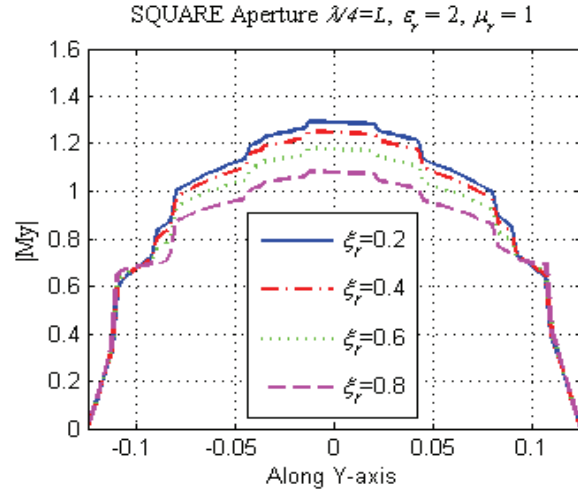


Fig. 7. Equivalent magnetic current with different chiralities.

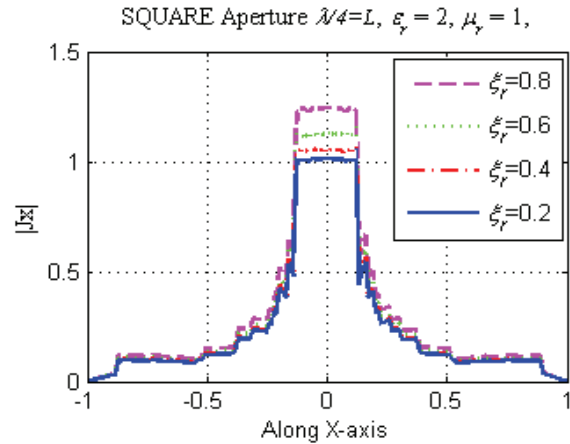


Fig. 8. Equivalent electric current with different chiralities.

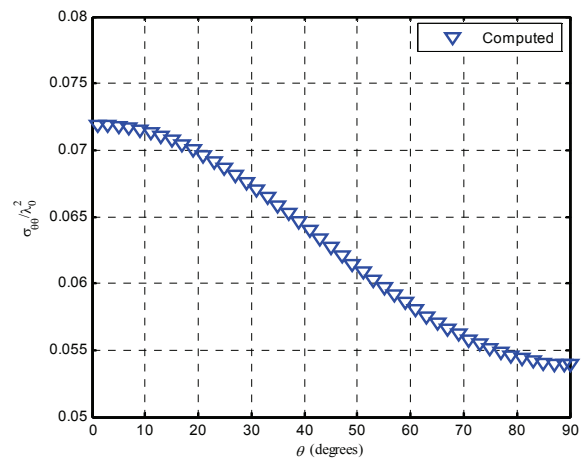


Fig. 9. $\sigma_{\theta\theta}$ of square aperture with $\xi_r = 0.4$, $\varepsilon_r = 2$, $\mu_r = 1$.

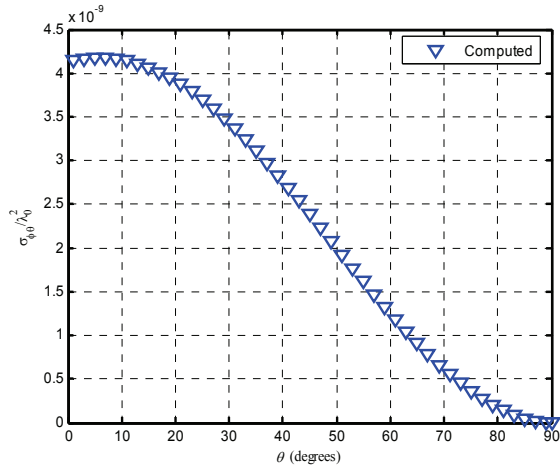


Fig. 10. $\sigma_{\phi\theta}$ of square aperture with $\xi_r=0.4$, $\epsilon_r=2$, $\mu_r=1$.

$-E_x / E^{inc}$ approaches the phase of M_y / E^{inc} in the aperture in Fig. 6. In Fig. 13, $|E_y / E^{inc}|$ is well below $|E_x / E^{inc}|$ as expected. Figures 14 and 15 show $|E_x / E^{inc}|$ and $|E_y / E^{inc}|$ when $\xi_r=0.5$.

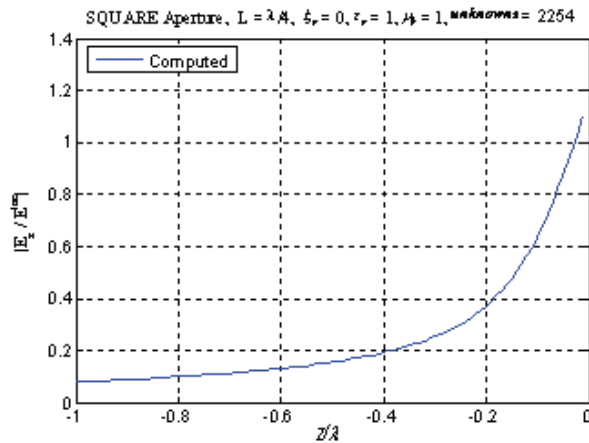


Fig. 11. $|E_x / E^{inc}|$ in Region b behind aperture when $\xi_r=0$.

Figure 16 shows the transmission cross section patterns, τ_θ in the $x=0$ plane, and τ_ϕ in the $y=0$ plane where,

$$\tau_\theta = 2\pi r^2 \left| \eta_0 H_\theta / E^{inc} \right|^2 \quad (11)$$

$$\tau_\phi = 2\pi r^2 \left| \eta_0 H_\phi / E^{inc} \right|^2 \quad (12)$$

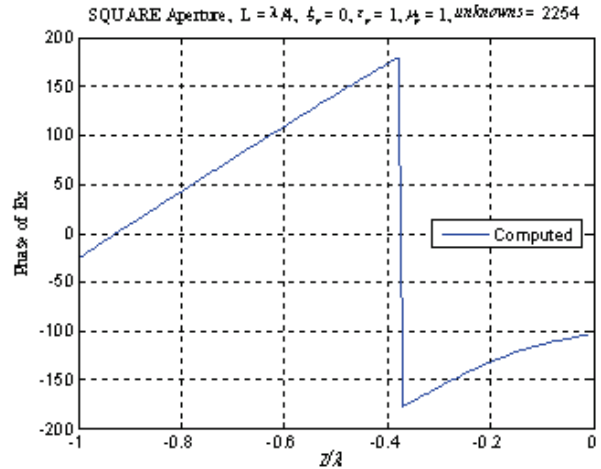


Fig. 12. Phase of \bar{E}_x in Region b behind aperture when $\xi_r=0$.

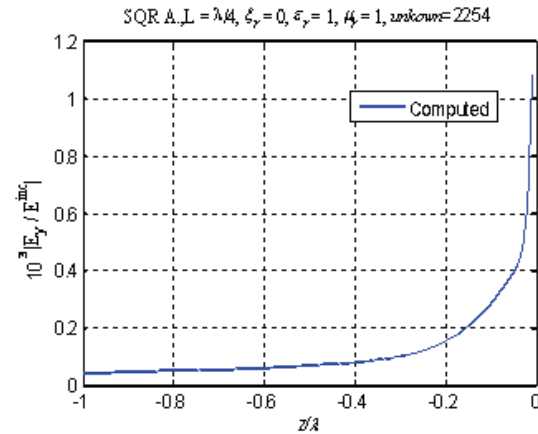


Fig. 13. $|E_y / E^{inc}|$ in Region b behind aperture when $\xi_r=0$.

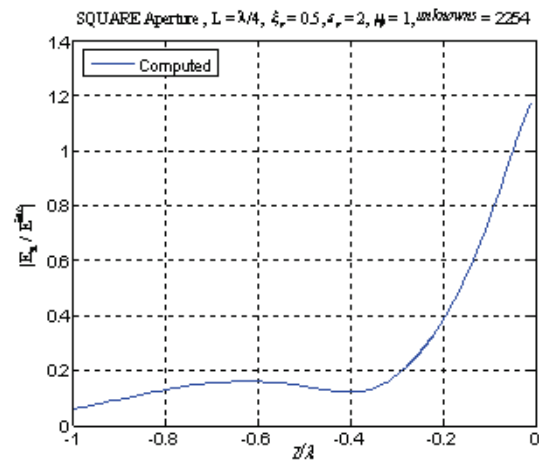


Fig. 14. $|E_x / E^{inc}|$ in Region b behind aperture when $\xi_r=0.5$.

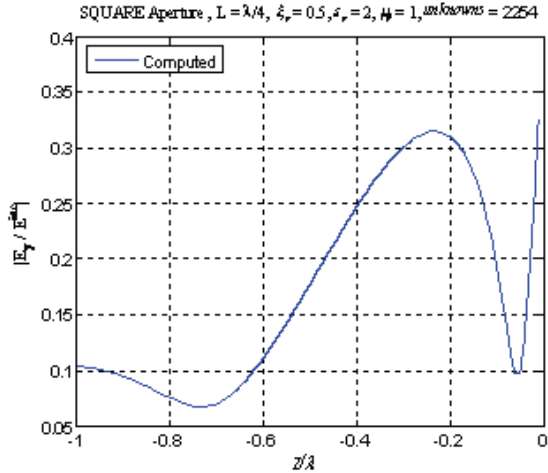


Fig. 15. $|E_y / E^{inc}|$ in Region b behind aperture when $\xi_r = 0.5$.

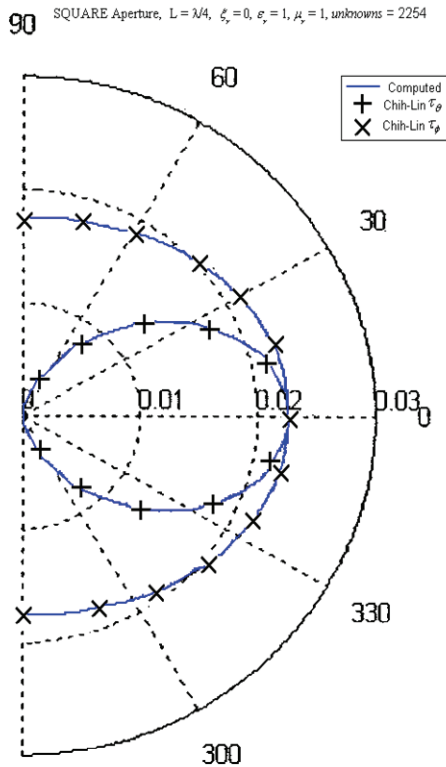


Fig. 16. Transmission cross section patterns when $\xi_r = 0$.

These patterns are in good agreement with those in [10]. Direct comparison with patterns shown in [11] is not possible because all patterns shown in [11] are for the dual problem of scattering by a rectangular plate. Figures 17 and 18 show the patterns with various chiralities. Table 1 shows the

transmission coefficient comparison results, which agree with those in [10], and also shows the change with various chiralities. The transmission coefficient is P_{trans} / P_{inc} . P_{trans} is the transmitted power going through the aperture. P_{inc} is the incident power in free space on the aperture.

$$P_{trans} = -\frac{1}{2} \text{Re} \int_{\text{apert.}} (\vec{E} \times \vec{H}^*) \cdot \hat{z} \, ds \quad (13)$$

$$P_{inc} = \eta |\vec{H}^{inc}|^2 S \cos \theta^{inc} \quad (14)$$

where S is the area of the aperture.

If the PEC plane was really finite, then, very far into the chiral material, the PEC plane would have no effect. As a result, only the effect of the incident field on the interface between air and the chiral material would be seen. This effect would mask any transmission cross section. However, because the left-hand side of (8) is obtained by using the infinite PEC plane, the PEC plane does not look small very far into the chiral material so that transmission cross sections can be obtained. Chiral materials are also used to reduce the radar cross section [12],[13].

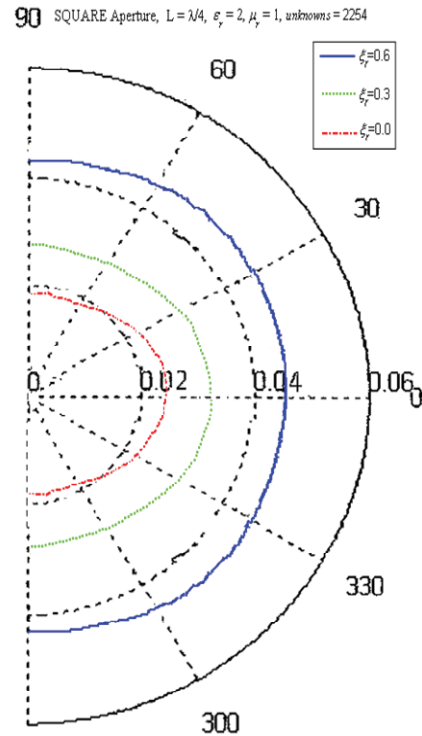


Fig. 17. Transmission cross section pattern (τ_ϕ) with various chiralities.

Table 1: Transmission coefficient for square aperture.

SQUARE APERT. $W=L=\lambda/4$	CHIH LIN I	COMPTD. ($\xi_r=0$)	COMPTD. ($\xi_r=0.3$)	COMPTD. ($\xi_r=0.6$)
APERT. AREA	0.0625 (λ^2)			
TRANS. COEFF.	0.21483	0.21228	0.33157	0.41391
TRANS. AREA	0.01342 (λ^2)	0.01326 (λ^2)	0.02072 (λ^2)	0.02586 (λ^2)

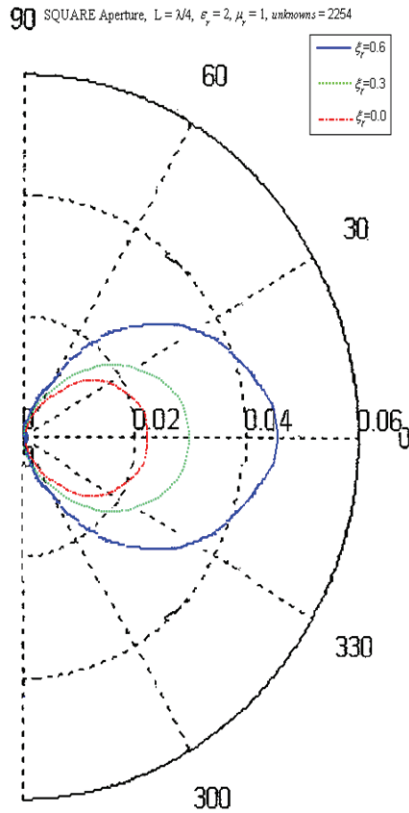


Fig. 18. Transmission cross section pattern (τ_θ) with various chiralities.

B. Slot Aperture

As a second check, an aperture which is a thin slot is meshed. The mesh starts fine and gets coarser near the edges of the finite conducting plane. The excitation is a normally incident unit

plane wave traveling in the $-z$ direction. The mesh is finer than that for the square aperture because of the thin width ($W = \lambda/20$) shape. This time, 3972 unknowns took 23 minutes on the same machine mentioned previously in Figs. 20–28, where the units along each horizontal axis are those of the ratio of length to wavelength, the units of M_y are those of the incident electric field and the phase of M_y is plotted in degrees. Three different slot lengths are considered. The width is always $\lambda/20$, but the lengths are $\lambda/4$, $\lambda/2$, and λ . In the case of the length $\lambda/2$, the magnetic current is large because of a resonance. When the chirality is equal to zero, the magnetic current magnitude and phase agree with those in [10] and [14] in all cases. Table 2, for which $\epsilon_r = \mu_r = 1$, gives transmission coefficients for $\xi = 0, 0.3$ and 0.6 . In Table 2, the computed transmission coefficients for $\xi_r = 0$ compare favorably with the transmission coefficients in [10].

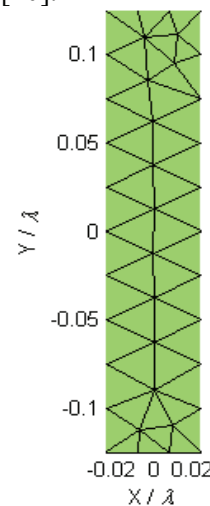


Fig. 19. Slot with $W = \lambda/20$ and $L = \lambda/4$.

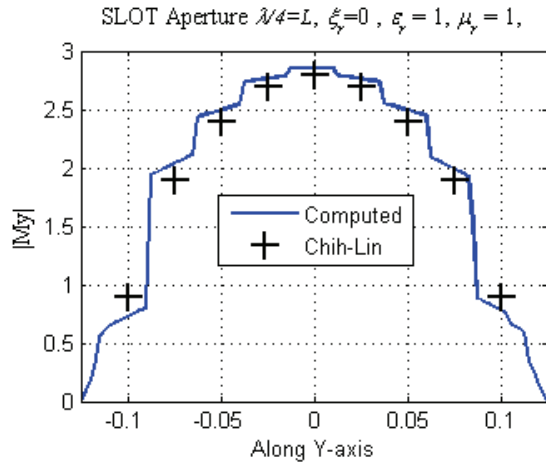


Fig. 20. Magnetic current comparison for slot aperture of $W = \lambda/20$ and $L = \lambda/4$.

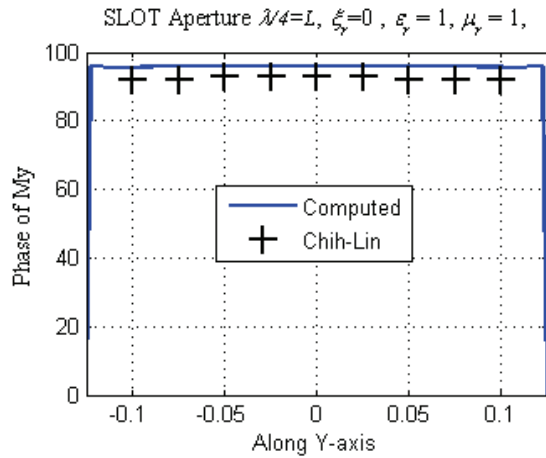


Fig. 21. Phase comparison for slot aperture of $L = \lambda/4$.

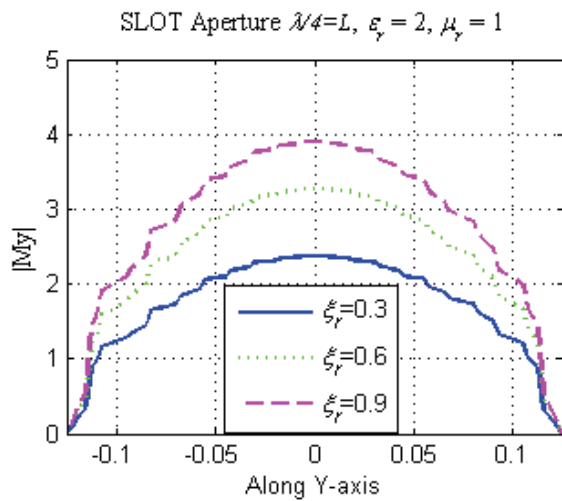


Fig. 22. Magnetic current with different chirality values.

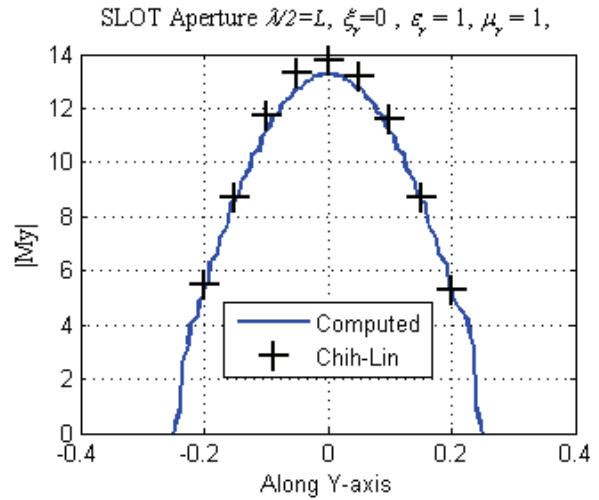


Fig. 23. Magnetic current comparison for slot aperture of $W = \lambda/20$ and $L = \lambda/2$.

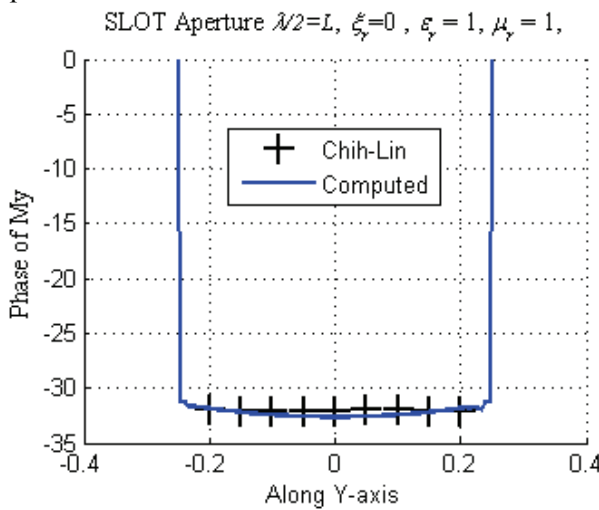


Fig. 24. Phase comparison for slot aperture of $L = \lambda/2$.

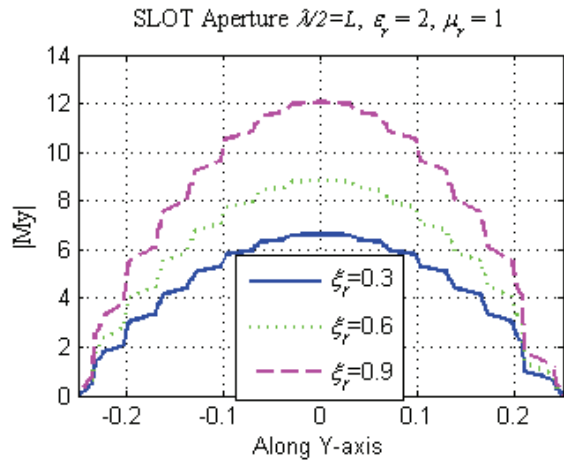


Fig. 25. Magnetic current with different chirality values.

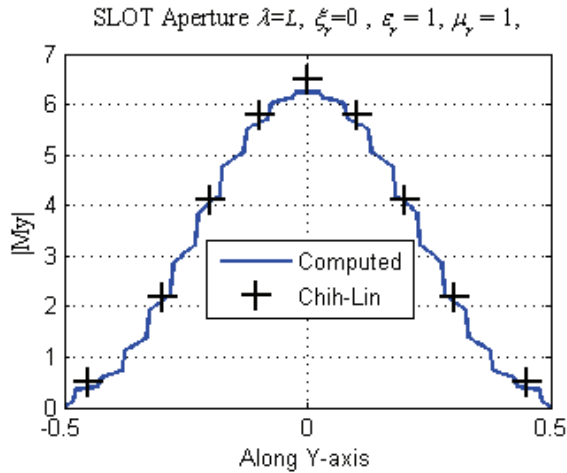


Fig. 26. Mag. current comparison for slot aperture of $L=\lambda$.

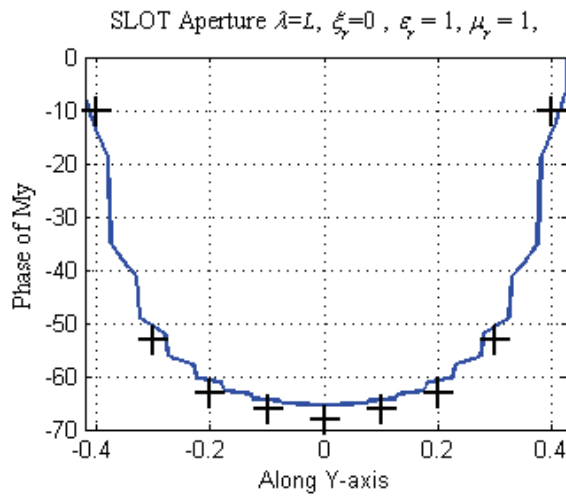


Fig. 27. Phase comparison for slot aperture of $L = \lambda$.

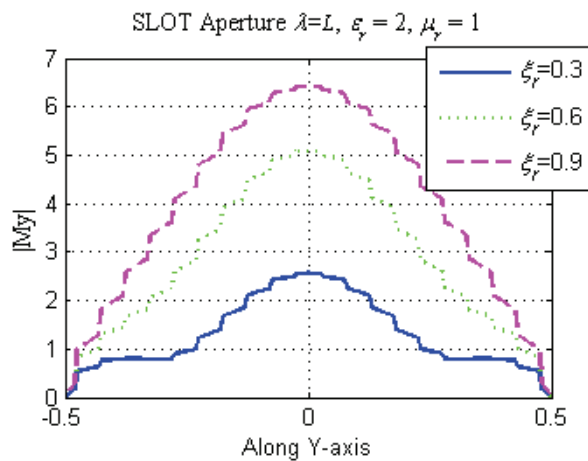


Fig. 28. Magnetic current with different chirality values.

Table 2: Transmission coefficient for slot aperture.

SLOT APERT. $W=\lambda/20$		CHIH LIN I [10]	COMPUTED $\xi_r=0$	COMPUTED $\xi_r=0.3$	COMPUTED $\xi_r=0.6$
$L=\lambda/4$	AP. AREA	0.012 $5(\lambda^2)$	0.012 $5(\lambda^2)$	0.012 $5(\lambda^2)$	0.012 $5(\lambda^2)$
	T. COEF	0.179	0.181	0.273	0.395
	T. AREA	0.002 $24(\lambda^2)$	0.002 $26(\lambda^2)$	0.003 $41(\lambda^2)$	0.004 $94(\lambda^2)$
$L=\lambda/2$	AP. AREA	0.025 (λ^2)	0.025 (λ^2)	0.025 (λ^2)	0.025 (λ^2)
	T. COEF	8.182	8.131	13.15	19.95
	T. AREA	0.204 $57(\lambda^2)$	0.203 $29(\lambda^2)$	0.328 $94(\lambda^2)$	0.498 $83(\lambda^2)$
$L=\lambda$	AP. AREA	0.05 (λ^2)	0.05 (λ^2)	0.05 (λ^2)	0.05 (λ^2)
	T. COEF	1.516	1.518	1.963	2.198
	T. AREA	0.075 $8(\lambda^2)$	0.075 $9(\lambda^2)$	0.098 $1(\lambda^2)$	0.109 $9(\lambda^2)$

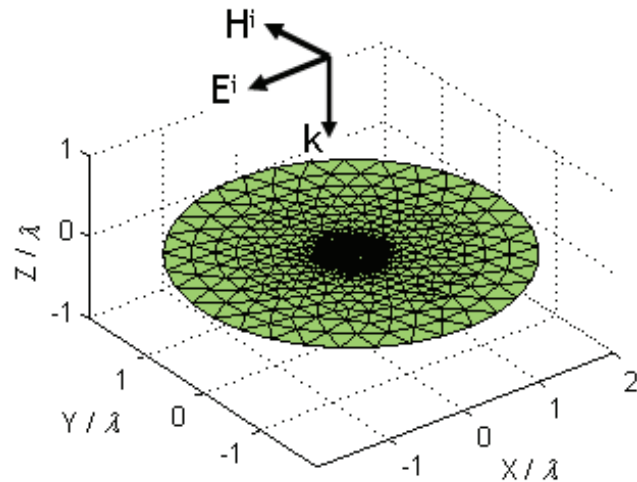


Fig. 29. Finite conducting plane with 2267 unknowns.

C. Circular Aperture

As a third check, a circular mesh is applied to a circular aperture. As it is seen in Fig. 29, the mesh

is fine at the edge of the aperture and is coarse at the end of the finite conducting plane. The incident

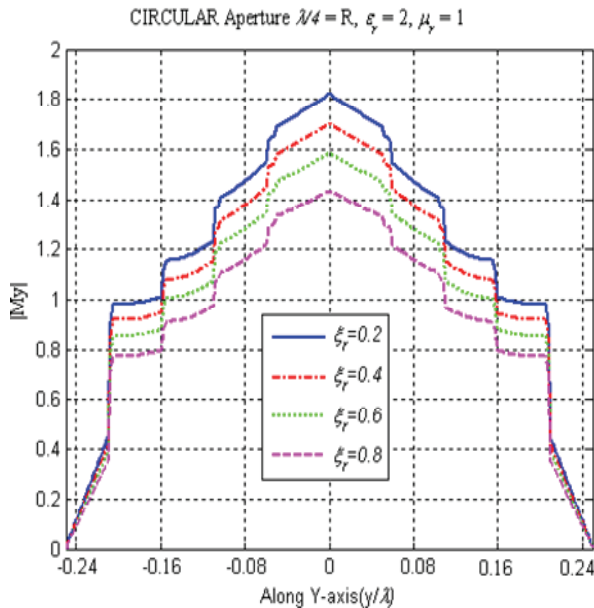


Fig. 30. Magnetic current with different chirality values.

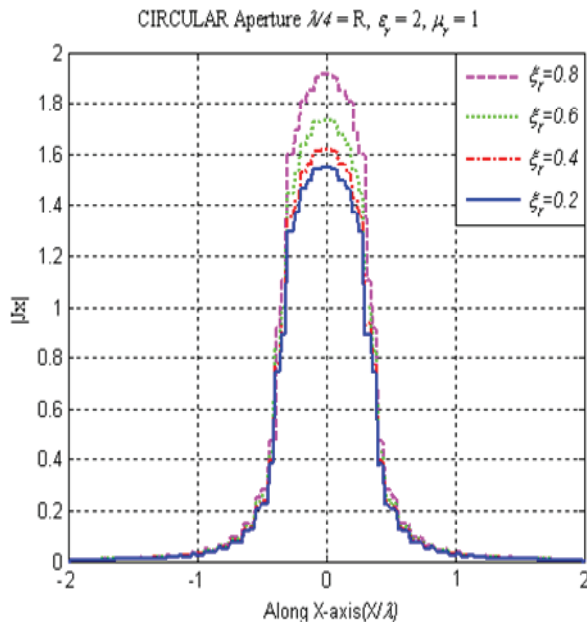


Fig. 31. Electric current with different chirality values.

field is again a normally incident unit plane wave traveling in the $-z$ direction. The radius of the aperture is $R=\lambda/4$. The mesh size is close to that of the square aperture. This time, 3267 unknowns took 19 minutes on the same machine mentioned previously. When the chirality is equal to zero, the

maximum value of the magnetic current agrees with that in [10]. In Figs. 30 and 31, the dominant components of the equivalent electric and the magnetic currents are plotted for various chiralities. The magnetic current decreases with increasing chirality as for the square aperture. Again chirality affects the current at the center of the aperture more than that at the edges.

V. CONCLUSION

In this work, the method of moments technique is used to solve the problem of transmission through an arbitrarily shaped aperture in a perfectly conducting plane separating air and a chiral medium. Excitation is assumed to be a plane wave. The equivalence principle is used to replace the aperture with a conducting surface with an equivalent magnetic current on each side of it. By enforcing the continuity of the tangential components of the total electric and magnetic fields across the aperture, coupled integral equations are obtained. Triangular patches have been used to model the current in the aperture and on the conductor. The equivalent magnetic currents are approximated by linear combinations of expansion functions. The mixed potential formulation for a homogeneous chiral medium is used to obtain the electric and the magnetic fields produced by these expansion functions. In the mixed potential formulation, the expression for the electric field of an electric current contains the electric scalar potential as well as the magnetic vector potential. The coefficients of these expansion functions are obtained by using the method of moments to solve the coupled integral equations.

ACKNOWLEDGMENT

The authors would like to thank S. Arvas, T. Yemliha and D. Worasawate for providing the meshing programs and the MoM codes.

REFERENCES

- [1] D. Worasawate, J. R. Mautz., and E. Arvas, "Electromagnetic scattering from an arbitrarily shaped three-dimensional homogeneous chiral Body," *IEEE Trans. Antennas Propagat.*, vol. 51, pp. 1077–1084, May 2003.

- [2] V. Demir, A. Z. Elsherbeni, and E. Arvas, "FDTD formulation for dispersive chiral media using the Z transform method," *IEEE Trans. Antennas Propagat.*, vol. 53, pp. 3374–3384, Oct. 2005.
- [3] F. Bilotti, A. Toscano, and L. Vegni, "FEM-BEM formulation for analysis of cavity-backed patch antennas on chiral substrates," *IEEE Trans. Antennas Propagat.*, vol. 51, pp. 306–311, Feb. 2003.
- [4] C. Christopoulos, J. Paul, and D. W. P. Thomas, "Simulation of EM wave propagation in magnetoelectric media using TLM," *Int. J. Numer. Model.*, vol. 14, pp. 493–505, 2001.
- [5] D. Worasawate, "Electromagnetic scattering from an arbitrarily shaped three-dimensional chiral body," *Ph.D. dissertation*, Syracuse University, 2002.
- [6] I. V. Lindell, A. H. Sihvola, S. A. Tretyakov, and A. J. Viitanen, *Electromagnetic Waves in Chiral and Bi-Isotropic Media*, Artech House, 1994.
- [7] K. A. Michalski, "The mixed-potential electric field integral equation (EFIE) for objects in layered media," *AEU*, vol. 39, pp. 317–322, Sept-Oct. 1985.
- [8] R. F. Harrington, *Time-Harmonic Electromagnetic Fields*, New York: McGraw-Hill, 1961
- [9] S. M. Rao, D. R. Wilton, and A. W. Glisson, "Electromagnetic scattering by surfaces of arbitrary shape," *IEEE Trans. Antennas Propagat.*, vol. AP-30, pp. 409–418, May 1982.
- [10] C. -L. I and R. F. Harrington, "Electromagnetic transmission through an aperture of arbitrary shape in a conducting screen," *Technical Report No. 16*, Syracuse University, April 1982.
- [11] K. Hongo and H. Serizawa, "Diffraction of electromagnetic plane wave by a rectangular plate and a rectangular hole in the conducting plate," *IEEE Trans. Antennas Propagat.*, vol. 47, pp. 1029–1041, 1999.
- [12] D. L. Jaggard and N. Engheta, "Chirosorb™ as an invisible medium," *Electronics Letters*, vol. 25, no. 3, pp. 173–174, Feb. 1989.
- [13] R. Sharma and N. Balakrishnan, "Scattering of electromagnetic waves from arbitrary shaped bodies coated with a chiral material," *Smart Materials and Structures*, vol. 7, no. 6, pp. 851–866, Dec. 1998.
- [14] R.F. Harrington and J.R. Mautz, "Electromagnetic transmission through an aperture in a conducting plane," *AEU*, vol. 31, pp. 81–87, 1977.



S. Taha İmeci received the B.Sc. degree in Electronics and Communications Engineering from Yildiz Technical University, Istanbul, Turkey in 1993, and the M.S.E.E. and Ph.D. Degrees from Syracuse University, Syracuse, NY in

2001 and 2007, respectively.

He was with Anaren Microwave Inc., East Syracuse, NY from 2000 to 2002, and Herley Farmingdale, New York from 2002 to 2003, and PPC, Syracuse, NY from 2003 to 2005, and Sonnet Software Inc., Liverpool, NY from 2006 to 2007. He was a teaching assistant in the Department of Electrical Engineering and Computer Science at Syracuse University from 2005 to 2006. He has authored an abstract, "A project-based graduate antenna course," *2003 IEEE International AP Symp.*, and *USNC/CNC/URSI North American Radio Science Mtng*, June 22–27, Columbus, OH, p. 454, *URSI Digest.*, and five conference papers, "A wide band 3dB Hybrid/Hopfer Coupler" at *Antem/URSI 2004*, July 20–23 Ottawa-Canada, "Electromagnetic transmission through an aperture in a conducting plane between air and a chiral medium" *Aces2008*, March 30th-April 4th, *Niagara Falls-Canada*, "Circularly Polarized Microstrip Patch Antenna with Slits", "20 dB Hybrid Stripline Coupler", "Corners Truncated Microstrip Patch Antenna", at *Aces2010*, April 26th-April 29th *Tampere, Finland*, and he has authored 5 conference papers in Turkey.

Dr. İmeci is a member of TMMOB, Chamber of Electrical Engineers in Turkey since 1993, and the Applied Computational Electromagnetics Society (ACES).

Fikret Altunkilic was born in Ordu, Turkey in 1970. He received the B.Sc. degree in Electronics and Communications Engineering from Istanbul Technical University, Istanbul, Turkey in 1996, and the M.S.E.E. and Ph.D. Degrees from Syracuse University, Syracuse, NY in 2003 and 2007, respectively. He is presently with Skyworks Solutions, Woburn, MA.

Joseph R. Mautz (S'66-M'67-SM'75-F'05-LF'05) was born in Syracuse, NY in 1939. He received the B.S., M.S. and Ph.D. Degrees in electrical engineering from Syracuse University, Syracuse, NY in 1961, 1965, and 1969 respectively.

Until July 1993, he was a Research Associate in the Department of Electrical and Computer Engineering of Syracuse University working on radiation and scattering problems. He is presently an adjunct professor in the Electrical Engineering and Computer Science Department at the same University. His primary fields of interest are electromagnetic theory and applied mathematics. He is a member of the Applied Computational Electromagnetics Society (ACES).

Ercüment Arvas (M'85-SM'89-F'03) received the B.S. and M.S. degrees from the Middle East Technical University, Ankara, Turkey in 1976 and 1979, respectively, and the Ph.D. degree from Syracuse University, Syracuse, NY in 1983, all in electrical engineering.

From 1984 to 1987, he was with the Electrical Engineering Department, Rochester Institute of Technology, Rochester, NY. In 1987, he joined the Electrical Engineering and Computer Science Department at Syracuse University where he is currently a Professor in the Electrical Engineering and Computer Science Department. His research and teaching interests are in electromagnetic scattering and microwave devices.

Prof. Arvas is a member of the Applied Computational Electromagnetics Society (ACES).